Iron supply to the western subarctic Pacific: Importance of iron export from the Sea of Okhotsk

Jun Nishioka[1,2], Tsuneo Ono [3], Hiroaki Saito [4], Takeshi Nakatsuka[1], Shigenobu Takeda[5], Takeshi Yoshimura[2], Koji Suzuki[6], Kenshi Kuma[7], Shigeto Nakabayashi[8], Daisuke Tsumune[2], Humio Mitsudera[1], W. Keith Johnson[9], Atsushi Tsuda[10]

[1]Pan-Okhotsk Research Center, Institute of Low Temperature Science, Hokkaido University, Sapporo, Hokkaido 060-0819, Japan

[2] Central Research Institute of Electric Power industry, Abiko, Chiba 270-1194 Japan

[3] Hokkaido National Fisheries Research Institute, Kushiro, Hokkaido, 085-0802 Japan

[4] Touhoku National Fisheries Research Institute, Shiogama, Miyagi, Japan 985-0001

[5] Department of Aquatic Bioscience, University of Tokyo, Bunkyo, Tokyo 113-8657, Japan

[6]Faculty of Environmental Earth Science, Hokkaido University, Sapporo, Hokkaido 060-0810, Japan

[7]Faculty of Fisheries Science, Hokkaido University, Sapporo, Hokkaido 060-0813, Japan

[8] Japan Agency Marine-Earth Science and Technology, Yokohama, Kanagawa 237-0061, Japan

[9]Climate Chemistry Laboratory, Institute of Ocean Sciences, Fisheries and Oceans Canada, PO Box 6000, Sidney, BC, V8L 4B2, Canada

[10]Ocean Research Institute, University of Tokyo, Nakano, Tokyo 164-8639, Japan

Correspondence and requests for materials should be addressed to Jun Nishioka. (e-mail: nishioka@lowtem.hokudai.ac.jp)

Abstract

Iron is an essential nutrient and plays an important role in the control of phytoplankton growth [Martin et al.,1989]. Atmospheric dust has been thought to be the most important source of iron, supporting annual biological production in the Western Subarctic Pacific (WSP) [Duce and Tindale, 1991; Moore et al., 2002]. We argue here for another source of iron to the WSP. We found extremely high concentrations of dissolved and particulate iron in the Okhotsk Sea Intermediate Water (OSIW) and the North Pacific Intermediate Water (NPIW), and water ventilation processes in this region probably control the transport of iron through the intermediate water layer from continental shelf of the Sea of Okhotsk to a wide areas of the WSP. Additionally, our time-series data in the Oyashio region of the WSP indicates that the pattern of seasonal changes in dissolved iron concentrations in the surface mixed layer was similar to that of macronutrients, and that deep vertical water mixing resulted in higher winter concentrations of iron in the surface water of this region. The estimated dissolved iron supply from the iron rich intermediate waters to the surface waters in the Oyashio region was comparable to or higher than the reported atmospheric dust iron input and thus a major source of iron to these regions. Our data suggests that the consideration of this source of iron is essential in our understanding of spring biological production and biogeochemical cycles in the western subarctic Pacific and the role of the marginal sea.

1. Introduction

Mesoscale iron enrichment experiments conducted in the western and the eastern subarctic Pacific clearly reveal that iron limits phytoplankton growth, especially during the summer, in these two areas [Tsuda et al., 2003; Boyd et al., 2004]. Previous studies reported that the eastern subarctic Pacific (ESP) oceanic time series station showed little seasonal variation in phytoplankton increase [Boyd and Harrison, 1999]. In contrast, the western subarctic Pacific (WSP) is often more productive in its lower trophic levels, especially during the bloom season from spring to summer in the Oyashio region [Saito et al., 2002]. A very large biological drawdown of pCO_2 in the WSP was also observed during this period [Takahashi et al., 2002]. Since iron limits phytoplankton growth during the summer in the WSP, there are considerable interests in determining the source and seasonal timing of iron input, which can lead to a steady spring phytoplankton bloom as found in the Oyashio region. A previous study indicates that there is a longitudinal dust gradient across the North Pacific, that is, the flux of dust containing iron over the WSP is an order of magnitude higher than in the ESP [Duce and Tindale, 1991]. This is due to the closer proximity to the second largest dust source in the world, the Gobi Desert, and this has been believed to be the leading cause for the longitudinal differences in biological production between the WSP and the ESP. A recent study by Uematsu et al. [2003] has reported that a numerical model simulation successfully reproduced the variation of mineral aerosol concentrations and total deposition flux over the western North Pacific and Measures et al. [2005] showed that dust fluxes, which were estimated based on dissolved Al concentrations in surface water, are significantly lower than those estimated by the previous study of Duce and Tindale [1991]. However, the role of iron dust supply to stimulate biological production has not been well quantitatively evaluated due to lack of information on the fraction of atmospheric iron that is bioavailable [Jickells et al, 2005]. Alternatively Brown et al. [2005] suggested that upwelling dominates the supply of dissolved iron to surface

72 waters north of 45 0N in the WSP. Additionally, previous studies indicate that re-
73 suspended particles from continental shelf sediments are postulated as a primary source
74 of iron for phytoplankton [Wells and Mayer, 1991; Croot and Hunter, 1998; Johnson et
75 al., 1999; Bruland et al., 2005; Chase et al., 2005; Elrod et al., 2004], and that these
76 iron-containing particles can be transported over long distances by eddies and water
77 current systems [Wu and Luther, 1996; Johnson et al., 1997; Löscher et al., 1997; Wells
78 et al., 1999; Johnson et al., 2005; Lam et al., 2006]. To date, however, the importance
79 of iron supply processes from the continental shelf by water current transport has not
80 been argued before for in the WSP.

81 Physical properties of each water mass in the WSP are complex and are strongly
82 influenced by a marginal sea, the Sea of Okhotsk. A schematic drawing of the
83 ventilation and water current system in the WSP can be found in Figure 1. The Sea of
84 Okhotsk is a marginal sea located on the northwest rim of the Pacific Ocean and is
85 known to be the lowest latitude seasonal sea ice area in the world [Alfultis and Martin,
86 1987; Kimura and Wakatsuchi, 2000]. Every winter, large amounts of sea ice are
87 produced along the Siberian coast on the north-western continental shelf of the Sea of
88 Okhotsk (shallower than 400 m depth) as a result of the cold winter winds blowing in
89 from East Siberia coupled with the fresh water discharge from the Amur river. The sea
90 ice formation rejects a large volume of cold brine, and subsequently the brine water
91 settles on the bottom of the north-western continental shelf along the Siberian coast to
92 form Dense Shelf Water (DSW: 26.8-27.0σ_θ) [Martin et al., 1998; Gladyshev et al.,
93 2000]. Because the density of the DSW generally does not exceed 27.0σ_θ, reflecting the
94 low salinity of surface water, the DSW does not sink to the bottom of the open sea, but
95 tends to penetrate the upper layer (250 ~ 450 m depth) of the Okhotsk Sea intermediate
96 water (OSIW) [Wong et al., 1998; Itoh et al., 2003; Yamamoto-Kawai et al., 2004].
97 The OSIW flows southward along the East Sakhalin coast, and is further exported
98 through “Bussol Strait” into the North Pacific Ocean after strong vertical diapycnal

mixing in the Kuril Straits [Nakamura and Awaji, 2004]. Thus, the OSIW contributes to the formation of the North Pacific Intermediate water (NPIW) [Tally, 1991; Yasuda, 1997; Nakamura and Awaji, 2004; Nakamura et al., 2006]. Thus the waters properties of the Oyashio region are strongly influenced by the intermediate water originating in the Sea of Okhotsk. On the other hand, the WSP off the east coast of Japan is a crossroads of water masses that are carried by the Kuroshio, the Oyashio and eddies (Figure 1). The Kuroshio transports a large amount of warm saline water into the midlatitude Ocean. The Oyashio is the western boundary current of the western subarctic gyre which is formed by cold, fresh water being transported along the east side of the southern Kuril Island [Nakamura et al., 2006; Yasuda et al., 2001]. The Oyashio current flows southward along the northeast coast of Japan as far as 30-40º N, then turns eastward and mixes with warm saline subtropical Kuroshio water. The Subarctic Front (SF: temperature front) is formed at the Oyashio-Kuroshio inter-frontal region (Figure 1).

Nakatsuka et al., [2002; 2004] pointed out that, in the Sea of Okhotsk, there is an efficient system of sediment material transport from the north-western continental shelf to the open sea via intermediate water transportation (DSW, OSIW). Other studies also found that injections of large amounts of POC and DOC from the Sea of Okhotsk led to increased DOC concentrations in the NPIW [Hansell et al., 2002; Hernes and Benner, 2002]. Extrapolating from these previous studies, it is possibile that iron would also be transported by the intermediate waters from the continental shelf of the Sea of Okhotsk to wide area of the WSP. In this study, we investigate, 1) iron transport process from the continental shelf of the marginal sea to the WSP by an intermediate water ventilation and 2) the seasonal variability of dissolved iron concentrations from winter to late spring (including the natural spring bloom period) in the Oyashio region. Then, we argue for the possibility of the influence of this source of iron on the spring bloom in

125 the Oyashio region, which is one of the highest biological productive areas in the world
126 oceans.

127

128 **2. Methods**

129 **2.1. Observations around the Kuril Islands**

130 Seawater sampling was conducted from the R/V *Mirai* to observe spatial
131 distributions of iron in the WSP and the southern part of the Sea of Okhotsk in May to
132 June 2000. The observation stations are indicated with triangles in Figure 1. To
133 characterize vertical profiles of iron concentration, seawater samples and hydrographic
134 data were collected using a clean CTD-carousel multiple sampler (CMS, SBE-911plus
135 and SBE-32 water sampler, Sea Bird Electronics, Inc.) system which housed twelve
136 acid cleaned Teflon coated 12-L Niskin-X bottles. For sub-sampling from the Niskin-X
137 sampler, 0.22 μm Durapore filters (Millipac 100, Millipore Corp.) were connected to
138 the Niskin-X spigot, and the filtrate was collected in acid-cleaned 125-ml LDPE bottles
139 (Nalgene Co., Ltd) under gravity pressure. The filtrate and unfiltered samples were
140 adjusted to pH 3.2 with addition of 2.4 M ammonium -10 M formic buffer, and
141 "dissolved iron" (that is, leachable iron in 0.22 μm filtrate at pH 3.2) and "total
142 dissolvable iron" (that is, dissolved plus leachable iron in unfiltered sample at pH 3.2)
143 were analyzed onboard by FIA chemiluminescence detection system [Obata et al.,
144 1993]. It should be noted that acidification to pH 3.2 is not sufficient to release all the
145 iron from particulate forms [Obata et al., 1997]. For this cruise, the samples were
146 allowed to sit at pH 3.2 for approximately 24 hours at room temperature to allow for a
147 weak digestion of particulate matter resulting in analysis of what we have defined as
148 "total dissolvable iron". Therefore, "total dissolvable iron" in this study only includes
149 the iron leached at pH 3.2 for 24 hour. All sample treatments were performed in a

laminar flow clean-air hood in a clean-air laboratory. Nutrients concentrations were also analysed in water samples collected from the same stations.

2.2. Observations for seasonal variation of iron concentration in the Oyashio region

Time-series observations were carried out monthly from January to the end of May, 2003, along the observation line of the National Fisheries Research Institute (*A-line* [Saito et al., 2002]) which crossed the Oyashio current (Figure 1) in the WSP (stations indicated by filled circles in Figure 1). During five cruises by the the following research vessels, Hokko-Maru in January (15 – 22 January), Oshoro-Maru in February (10–14 February) and March (11–20 March), and Wakataka-Maru in April (11–25 April) and May (7–19 May), samples were collected from surface to 800 m maximum with one to seven stations sampled regularly along the *A-line* (Table 1). During the April and May cruises, we visited *A-line* twice in each cruise, with sampling conducted at the beginning and end of each cruise. Samples to investigate temporal variability were also collected at oceanic station KNOT (44 ºN, 155 ºW, B9 in Figure 1) during March, April and May. Additionally, in the April and May cruises, seawater sampling was conducted to observe spatial distributions of iron in the WSP at the stations indicated by open circles in Figure 1. Seawater samples for this set of observations were collected using acid cleaned Teflon coated 10-L Niskin-X bottles suspended on Kevlar line. The unfiltered samples were adjusted to pH <1.8 with addition of 0.05 M of HCl, and the filtrate were adjusted to pH 3.2 with addition of 2.4 M ammonium -10 M formic buffer. Our defined “dissolved iron” concentrations (that is, leachable iron in 0.22 μm filtrate at pH 3.2) were analysed onboard and “total iron” concentrations were measured after more than 1 year storage by FIA chemiluminescence detection system (that is, dissolved plus leachable iron in unfiltered sample at < pH 1.8 during more than 1 year storage). All sample treatments were performed in a laminar flow clean-air hood

177 in a clean-air tent. Nutrients and chlorophyll *a* concentrations were also analysed for
178 water samples. Hydrographic data was also collected at all stations using a CTD.
179
180 **2.3. Observations of a longitudinal section of iron profiles in the North Pacific**
181 **along 165º E**
182 A longitudinal vertical section observation in the North Pacific along 165º E was
183 carried out (stations indicated filled square in Figure 1) in September 2003 by Hakuho-
184 maru KH03-2 cruise. Seawater samples for total iron, dissolved iron, other chemical
185 measurement and hydrographic data were collected using a clean CTD-CMS system as
186 described in Section 2.1. "dissolved iron" and "total iron" concentrations were
187 measured as described in Section 2.2.
188
189 **2.4. Iron analysis in this study**
190 Concentrations of Fe (III) in buffered and acidified samples were determined using an
191 automatic Fe (III) analyzer (Kimoto Electric Co. Ltd.) using chelating resin
192 concentration and chemiluminescence detection [Obata et al., 1993]. The detection
193 limit (three times the standard deviation of Fe (III) concentrations for purified seawater,
194 which was passed through an 8-quinolinol resin column three times to remove Fe) was
195 0.017 to 0.032 nM (among the cruises). The relative standard deviation was within
196 4.2 % (n=34) for replicate measurements of a reference seawater sample containing
197 0.54 nM Fe (III). Our iron measurement method and reference seawater were vetted by
198 using SAFe (Sampling and Analysis of Iron) cruise [Johnson et al. 2007] reference
199 standard seawater (distributed by Moss Landing Marine Laboratory (MLML) for an
200 inter-comparison study) several years later, with our results comparing favourably for
201 dissolved iron concentration in ~ 0.1 nM and ~ 1 nM (MLML reference standard

202 seawater containing 0.099 nM and 0.91 nM iron were measured to be 0.10 ± 0.010 nM
203 (n=3) and 0.99 ± 0.023 (n=3) by our method, respectively (the reference seawater was
204 analysed on Dec. 26, 2006)).

205

206 **3. Results and Discussion**

207 **3.1. Iron export from the Sea of Okhotsk to the western subarctic Pacific**

208 Total dissolvable and dissolved iron concentrations around the Kuril Islands were
209 measured, and vertical profiles of iron and dissolved oxygen in the WSP, the Oyashio
210 region and the Sea of Okhotsk are shown in Figure 2 (a, b and c). Total dissolvable and
211 dissolved iron versus density plots are also shown in Figure 3 (a and b). The dissolved
212 iron profiles on the WSP side of the Kuril Islands showed nutrient-type distributions
213 with low iron concentrations in surface waters (< 0.1 nM), and extremely high
214 concentrations (~ 1.5 nM in dissolved iron) in the intermediate layer (maximum at 500-
215 800 m) (Figure 2a). These dissolved iron concentrations in the intermediate waters in
216 the WSP are approximately three times higher than that maximum concentration found
217 in the ESP (0.6 nM) [Nishioka et al., 2001]. Similarly, the intermediate water iron
218 concentrations in the Oyashio region were higher than that of open-ocean stations (B9
219 and C11) (Figure 2b). Meanwhile, in the Sea of Okhotsk, dissolved iron was
220 substantial in the surface mixed layer (0.2 ~ 0.6 nM), and obviously it showed much
221 higher total dissolvable iron concentrations (~ 10 nM) in the intermediate layer than
222 found in the WSP side (Figure 2c). Regarding the fractions of iron, maximum depths
223 for total dissolvable iron are shallower than that of dissolved iron in all profiles, and the
224 maximum depths for dissolved iron corresponds to the minimum depth for dissolved
225 oxygen (Figure 2 a, 2b and 2c). This is probably caused by sinking and
226 remineralization of particulate iron. The density of iron-rich intermediate waters in the

227 Sea of Okhotsk observed in this study obviously correspond to the density range of the
228 DSW and the OSIW (Figure 3a and 3b). It has been reported that the Oyashio region
229 waters originate partly from Sea of Okhotsk water with 26.6-27.5 σ_θ [Yasuda et al.,
230 2001] and that this density range also corresponds to the iron-rich intermediate waters
231 (NPIW) in the Oyashio region and the other region of the WSP (Figure 3a and 3b).
232 These our data suggests that substantial iron was exported along with the intermediate
233 water discharge from the Sea of Okhotsk to the WSP.

234

235 **3.2. Lateral iron transportation via intermediate water ventilation**

236 A longitudinal section of salinity, dissolved iron and total iron profiles in the North
237 Pacific along 165º E are shown in Figure 4a, 4b and 4c. Vertical profiles of dissolved
238 iron, total iron, salinity and dissolved oxygen at 35 ºN, 165º E are also shown in Figure
239 5. These longitudinal sections clearly indicate that high iron concentrations extend
240 southward at intermediate water depths (26.6-27.5 σ_θ). A low salinity intermediate
241 water mass, which was influenced by NPIW formation in the subarctic corresponds to
242 the iron-rich water mass (Figure 4a, 4b and 4c, Figure 5). Maximum depth of dissolved
243 iron corresponds to the minimum depth in dissolved oxygen (at 35 ºN, 165º E; Figure 5)
244 indicating remineralization processes as mentioned above. Watanabe et al. [1994]
245 reported that apparent ages for the NPIW along 175 ºE as by measured
246 chlorofluorocarbons in the North Pacific, and that NPIW is laterally transported
247 between subpolar and subtropical regions on timescales of a few decades. Therefore,
248 iron is transported by NPIW from the subarctic region to subtropical region within a
249 few decades. Moreover, we observed a high total iron core in the intermediate water at
250 35 ºN (Figure 4c). Watabnabe et al. [1994] also suggested that NPIW (greater than
251 26.80 σ_θ) near 37 º N was older than its surrounding waters and that new NPIW formed
252 in the subpolar region is not transported directly southward. Additionally, a previous

253 physical modelling study pointed out that core of the Oyashio flow, which is
254 constructed of subarctic water, intrudes into the intermediate layer (around $27\sigma_\theta$ or 800-
255 1000 m) below the Kuroshio extention after the Oyashio flow turns eastward between
256 30-40 º N off the coast of Japan (Figure 1) [Mitsudera et al., 2004]. The high total iron
257 core in the intermediate water at 35º N might be induced by the Oyashio water pathway.

258 On the other hand, we observed high total iron in the bottom water in north of the
259 study region along 165º E (Figure 4c). It is likely that the northward increasing trend in
260 the iron levels in the bottom water is due to the effect of sinking particles of strong
261 biological productivity at high latitude, and southward advection and/or mixing of this
262 iron-rich bottom water occurred.

263 Our data described above suggest that the intermediate water masses, in the Sea of
264 Okhotsk (OSIW) and the WSP (NPIW), are extremely rich in dissolved and particulate
265 iron, and that water ventilation processes in this region control the transport of dissolved
266 and particulate iron through the intermediate water layer from the Sea of Okhotsk to a
267 wide areas of the WSP.

268

269 **3.3. Source of iron in the intermediate water**

270 It has been reported that the DSW, which is a source water of the OSIW,
271 consistently contains large amounts of re-suspended sedimentary particles, due to strong
272 tidal mixing on the shelf of the Sea of Okhotsk [Nakatsuka et al., 2002], and that the
273 outflow of DSW results in a large flux of particulate and dissolved organic matter (POC
274 and DOC) from the shelf to the OSIW [Nakatsuka et al., 2004]. Finally, the OSIW
275 transports the POC and DOC into the NPIW [Hansell et al., 2002; Hernes and Benner,
276 2002; Nakatsuka et al., 2004]. Another report has indicated that the OSIW has
277 extremely low N* value (($[NO_3^-]$-16*$[PO_4^{3-}]$+2.9)*0.87) due to the denitrification (or

exudation of phosphate) of anoxic pore water in the sediment of the north-western shelf region of the Sea of Okhotsk, and can act as a conservative tracer of the water [Yoshikawa et al., 2006]. Vertical profiles of iron and N* in the Sea of Okhotsk (station C1) and Oyashio region (C5) are shown in Figures 6a and 6b. Our data show that the iron-rich intermediate water masses clearly have low N* values in the Sea of Okhotsk (Figures 6a for station C1), and that this feature is also found in the water column of the Oyashio region (Figure 6b for staiton C5). In 2006 summer, we conducted direct observation in the north-western continental shelf area of the Sea of Okhotsk, and detected extremely high total iron concentration (> 60 nM) in original seawater of the DSW (data not shown) and Fe (II) in the pore water of the sediments (Minami, personal communication). These previous reports and our data imply that the large amounts of dissolved and particulate iron in the OSIW would be introduced by the re-suspension of the sediments from the north-western continental shelf area of the Sea of Okhotsk.

There is one more possible source of iron for the NPIW in the Oyashio region. Amakawa et al. [2004] reported neodymium isotopic data that the radiogenic Nd ultimately derived from volcanic provinces as the Kuril-Kamchatska and Aleutian islands is transported by the Oyashio current to form the NPIW. A recent study also reports that subduction zone volcanic ash has high iron concentrations [Duggen et al., 2007]. Therefore, coastal sediments of the Kuril Islands might be another source of the iron in the NPIW.

3.4. Spatial and temporal distributions of iron in the WSP

Our vertical measurements of iron in the WSP confirm previous observations that increased gradients in dissolved iron concentrations with depth from subsurface to

intermediate water (NPIW) were greater in the WSP [Fujishima et al. 2001, Nishioka et al., 2003, Brown et al., 2005] relative to that of the ESP. Furthermore, particulate iron was extremely high in the whole water column of the western region [Nishioka et al., 2003, Kinugasa et al., 2005, Brown et al., 2005]. However, the observations in this study also provide some new information on features of tempo-spatial variability of iron concentrations in the WSP. We found that extremely high total iron concentrations in the surface were observed only in subarctic water masses north of the SF, and that this feature was clearly separated by the SF border, which was as defined 6 oC in this study (Figure 7a, 7b and 7c). North of SF, there was a cold water mass which had extremely high total iron concentrations (Figures 7a, 7b and 7c) with the main form of iron being found in the particle phase (~ 80 %) (Figure 8 for Station A4). Conversely, high total iron concentrations were not observed in warm (> 6 oC) surface waters south of the SF as can be clearly seen in the profile of station B6 (Figure 8 for Station B6).

Additionally, time series iron observations of vertical profiles in the Oyashio region (A7) and at an oceanic station in the WSP (B9) clearly show that there was temporal variability in dissolved iron and total iron concentrations in the water column in both the regions (both the stations are located north of the SF) (Figure 9a and 9b). This variability was more pronounced than those of nitrate or salinity. Higher temporal variability of dissolved and total iron concentrations, especially in total iron, was observed in the entire water column in the Oyashio region (A7), upstream of the Oyashio flow and near the source of iron, than at the oceanic station (B9), downstream of the Oyashio flow (Figure 9a and 9b). These time-series data indicates that some fractions of the iron in particulates and colloidal matters were lost from the water column during the water transportation.

From our spatial and temporal iron distributions, it can be inferred that the high iron input, mainly in the particulate phase, occurs north of the SF and upstream of the

328 Oyashio region, and the iron is subsequently distributed to the cold subarctic water in
329 the WSP area. The results are consistent with our data that the iron-rich water is
330 transported from the Sea of Okhotsk to the WSP (described in section 3.1), and cannot
331 be solely explained by aeolian dust supply over the study area.

332

333 **3.5. Changes in dissolved iron concentrations during a spring bloom in the Oyashio**
334 **region**

335 Changes in dissolved iron, nitrate, surface mixed layer depths (MLD) and
336 chlorophyll *a*, in the surface of the Oyashio region are shown in Figures 10a, 10b, 10c
337 and 10d. We found there to be clear seasonal variability of dissolved iron
338 concentrations in the surface mixed layer along the monitoring line *A-line* in 2003
339 (Figure 10a). High nutrient levels in the surface mixed layer occurred in winter (~ 25
340 μM nitrate) (Figure 10b), due to the deep vertical mixing (~ 200 m) in winter, which
341 delivered high nutrient subsurface water into the surface (Figure 10c). In spring,
342 thickness of the surface mixed layer decreased (Figure 10c) and the nitrate
343 concentration was drawn down to 2 ~ 10 μM nitrate (Figure 10b) due to biological
344 uptake in spring bloom (Figure 10d). During the observation period in 2003, seasonal
345 changes in dissolved iron level was similar to that of nitrate in the surface mixed layer.
346 The dissolved iron concentration observed in the surface mixed layer of the Oyashio
347 region reached a maximum in January, and kept high throughout winter (ave. 0.6 nM).
348 As the development of the spring phytoplankton blooms, the dissolved iron levels
349 decreased to < 0.2 nM (Figure 10a). Higher surface dissolved iron concentrations in

March (~0.3 nM) compared to May (< 0.1 nM) were also observed in the oceanic region (B9) (Figure 9b).

Three sources can be proposed for explaining the relatively high dissolved iron levels in the surface mixed layer before the phytoplankton bloom in the Oyashio region: 1) input of soluble aerosol iron, 2) lateral transport into the surface layer and 3) turbulent vertical mixing of dissolved iron from the subsurface layer. Regarding 1), mineral dust and particulate pollutants from the Asian continent are transported eastward over the North Pacific, especially in spring [Uematsu et al., 1983]. Recently, significant temporal variability of iron concentrations in near surface waters at station HOT-ALOHA in the central North Pacific, one of the most intensely studied site for iron in the ocean, was reported by Boyle et al. [2005]. They indicated that the highest observed iron concentrations was seen during the period of peak Asian dust transport in spring season, and suggest that significant inter-annual differences in near-surface iron will occur as a result of inter-annual variability in Asian dust transport. The observed frequencies of dust events in 2003 were 0 day both in January and February, 6 days in March, 7 days in April and 2 days in May (these observations were performed by Japan meteorological agency at 98 meteorological stations on Japan using visually transmittance survey [http://www.data.kishou.go.jp/obs-env/kosahp/kosa_table_1.html]). In this study, the monthly variation (seasonality) of the dust events was clearly inconsistent with the seasonal change in dissolved iron in the surface mixed layer of the Oyashio region in 2003. Hence, the aeolian dust input would be a minor process for the phenomenon. However, occasionally surface maxima of dissolved and total iron can be found in vertical profiles of our data (e.g. Figure 9; station A7 January and station B9 March), which can not be explained by the vertical mixing of iron-rich intermediate water. Atmospheric input of mineral dust is one potential sources that could explain these surface maxima events.

As for 2), previous studies clearly indicated that strong vertical mixing occurs around the Kuril Straits. The diapicnal mixing around Kuril Straits strongly affects the temperature and salinity properties of the OSIW [Tally et al., 1991; Wong et al., 1998; Yamamoto et al., 2002]. Nakamura and Awaji [2004] performed numerical experiments to study tidally generated internal waves in the Kuril Straits and showed that tidal mixing was able to reach down to the OSIW. These previous studies suggest that the iron-rich intermediate waters probably influence the surface layer around the Kuril Straits and thus raise the MLD iron concentrations with subsequent transport to the Oyashio region. These theories cannot be verified using our data, unfortunately, but can be crucial processes for iron distributions in the Oyashio region. Detailed seasonal investigations of iron concentrations with physical parameters around the Kuril Straits must be needed to estimate the surface lateral iron transport from the Kuril Straits to the Oyashio region. Lateral transport from the Kuril Straits is also a possible source that might explain the surface maxima described in 1).

Regarding 3), our time series data can support the importance of the upward flux of iron by deep winter mixing in this region. One of the proof or evidence for this is that the seasonal change in dissolved iron behaves similar to that of nitrate in the surface mixed layer. The dissolved iron to nitrate supply ratio from the subsurface layer are summarized for the Oyashio region (St. A11), WSP (St.B9) and ESP (St. Papa) [Nishioka et al., 2001] in Table 2 (the values are calculated from data which show in Figure 11). The ESP consistently contains 0.004 nM Fe/μM NO_3 in the subsurface gradient. On the other hand, Stations. A11 and B9 have significantly higher ratios (0.044, 0.052, respectively) than ESP. Winter vertical mixing in the Oyashio region and the WSP supplies more iron than in the ESP. A greater supply of macronutrients and

400 substantially higher seasonal nutrient utilization in the WSP and Oyashio region
401 [Tsurushima et al., 2002; Harrison et al., 2004], compared with ESP, could be explained
402 by a larger upward iron flux in the WSP and Oyashio regions.

403

404 **3.6. Estimation of annual upward iron flux**

405 The vertical distributions of dissolved iron concentrations in the Oyashio region,
406 WSP, and ESP were utilized to estimate the vertically transported iron amounts to the
407 surface waters by eddy diffusion, vertical advection and winter mixing in order to
408 determine the annual upward flux of iron into the surface mixed layer. Typical
409 dissolved iron profiles in winter and late spring at Station A11 (Oyashio region), B9
410 (WSP) and Papa (ESP: reported data [Nishioka et al., 2001]) are used for this estimation
411 (Figure 11).

412 A schematic drawing of evaluated upward iron transport processes are shown in
413 Figure 12.

414 We have employed a simple one-dimensional model by Martin et al. [1989] to
415 estimate the vertically transported iron amounts to the surface waters from spring to
416 autumn by vertical advection and eddy diffusion (F_1). We define the winter period as 5
417 months (150 days), therefore, the formula of F_1 is used as an estimation for the
418 remaining 215 days.

419 $$F_1 = W*R*215_{days} + Kz*(dFe/dz)*215_{days} \quad \mu mol\ Fe\ m^{-2}$$

420 (referenced by Martin et al. [1989])

421 Where W is the vertical velocity, with a value of 0.012 m/day being employed as per
422 Martin et al. [1989], in all regions, R is the mean concentration of dissolved iron in the

423 vertical gradient in the subsurface layer, and Kz is the coefficient of eddy diffusivity.
424 We used 5 m^2/day for Kz from Martin et al. [1989] for all regions, and calculated
425 dFe/dz (gradient in dissolved Fe with depth (μmol/m^4)) from our data set (Figure 11).

426 The winter water column of the Oyashio region is characterized by weak density
427 stratification from the surface to intermediate waters (Figure 11), due to the strong
428 influence of the NPIW. Therefore, the true Kz value would be higher than the value
429 used for our F_1 calculation. In consideration of this fact, we decided to use a simple
430 straight forward method to estimate the iron amounts transported by winter mixing (F_2).
431 According to the concept of isopycnal mixing model reported by Sarmiento et al. [1990],
432 an inventory of iron raised to the surface waters by winter mixing (F_2) was estimated as
433 follows.

434 $$F_2 = (C_1 - C_2) * D_1 \qquad \mu mol\ Fe\ m^{-2}$$

435 C_1 is the summer dissolved Fe concentration at the maximum depth of the winter mixed
436 layer. C_2 is dissolved Fe concentration in the summer surface mixed layer. D_1 is the
437 summer surface mixed layer depth. We used our observed data for C_1, C_2 and D_1
438 (Figure 11, Table 2). We also assumed that the inventory of iron raised to the surface
439 waters by winter mixing (F_2) include the iron transported by vertical advection and
440 eddy diffusion.

441 The annual total upward dissolved iron flux is estimated by summation of F_1 and F_2
442 (μmol Fe $m^{-2}yr^{-1}$).

443 These fluxes are summarized and presented in Table 2. An estimate of
444 atmospheric dust deposition reported by Fung et al. [2000], results of the ocean global
445 model including iron, suggest that the total atmospheric dust flux in the western North
446 Pacific is 929 μmol Fe $m^{-2}yr^{-1}$ (ave. value for 40ºN, 170ºE), and that the average

447 solubility of airborne iron within the mixed layer must be ~ 1 % to represent observed
448 distribution of High Nutrient Low Chlorophyll (HNLC) waters in the North Pacific
449 [Fung et al., 2000; Aumont et al., 2003]. If the atmospheric dust solubility is 1 %, the
450 upward iron flux from intermediate waters to the surface in the Oyashio region and
451 other parts of the WSP (Table 2), would be comparable to or larger than the atmospheric
452 dust flux (9.29 μmol Fe $m^{-2}yr^{-1}$). Moreover, the upward iron flux estimated is
453 significantly higher for the Oyashio region and the WSP than the ESP area, due to the
454 "rich iron in the subsurface-intermediate water" and "deeper winter vertical mixing"
455 [Suga et al., 2004] in the WSP. These simple calculations suggest that the upward iron
456 flux is particularly significant in the Oyashio region and other parts of the WSP, and
457 probably comparable to atmospheric iron input. If we compare our upward fluxes to
458 estimates from previous studies from other regions, the flux in the Oyashio region and
459 the WSP are comparable or lower than those reported in the Southern Ocean (53.6 μmol
460 Fe $m^{-2}yr^{-1}$ [Löscher et al., 1997], 12.9 μmol Fe $m^{-2}yr^{-1}$ [Croot et al., 2004]).

461 Uematsu et al. [2003] using numerical simulation study indicated that several
462 sporadic deposition event of mineral dust over the HNLC region during the spring will
463 increase the dissolved iron concentration in surface water, 0.3-0.6 nM increase in 50 m
464 deep mixed layer if dissolution of iron in mineral particle is 10%. Furthermore, resent
465 other study by Buck et al. [2006] reported wide range of airborne soluble iron flux (0.56
466 ~ 710 nmol Fe $m^{-2}day^{-1}$) supplied by several dust event to the east of Japan and further
467 north off the Sea of Okhotsk in the northwest Pacific Ocean, which are estimated with
468 onboard dust observation data and solubility experiment of aerosol iron. However,
469 there are still uncertainties in the quantitative evaluation especially in regard to
470 atmospheric iron fluxes and the fraction of atmospheric dust that is bioavailable.
471 According to previous reports, iron solubility from dust could be < 0.1 % ~ 10%
472 [Jickells and Spokes, 2001; Jickells et al., 2005]. Baker et al [2006] also reported that
473 iron solubility in dust varies as a function of the dust load. On the other hand, iron

474 concentrations in the intermediate water are also variable (See section 3.4), and
475 probably distributed heterogeneously. Therefore, we need more detailed studies to
476 compare these dissolved iron sources with quantitative evaluation by observation and
477 simulation studies with modelling including biogeochemical processes of iron in the
478 ocean and atmosphere.

479

480 **3.7. Possible iron supply system in the WSP**

481 Here we propose a hypothesis that one of the important sources of iron in the
482 WSP region is the transportation of iron-rich intermediate waters, which contain re-
483 suspended iron from the continental shelf areas of the Sea of Okhotsk to a wide area of
484 the WSP (Figure 13). Water ventilation processes in this region control the iron
485 transportation. This source of iron is supplied to the surface layer by diffusion and
486 strong winter turbulence mixing in the Oyashio region, and diapicnal mixing at the
487 Kuril Straits. The proposed process can explain the significant and steady increases in
488 phytoplankton biomass in the Oyashio region during spring, as a result of turbulent
489 winter mixing processes increasing surface iron concentrations in a timely fashion-
490 suitable for the spring phytoplankton bloom. The same is not true for sporadic iron
491 supply from airborne dust events. The physical dynamics of currents transporting iron
492 and the diffusing and winter mixing system should be considered as important sources
493 of iron when predicting natural spring phytoplankton blooms in Oyashio region.
494 Although the intermediate water iron transportation process explains external iron input
495 to a wide area of the WSP, the available iron is not sufficient for complete utilization of
496 upwelled nitrate in the HNLC region in the WSP. This is mainly due to the loss of iron
497 during water transport.

4. Conclusion

In conclusion, we indicate that the intermediate waters in the western subarctic Pacific (WSP) receive their primary source of iron through ventilation processes originating in the Sea of Okhotsk, a marginal sea. This source of iron is distributed to subarctic waters in the WSP area, and the form of the introduced iron is mainly in the particulate phase. Furthermore, there is a clear seasonality in dissolved iron concentrations in the surface waters of the Oyashio region. The waters are significantly influenced by high iron concentrations in the intermediate waters through diffusion and winter mixing. Therefore, in addition to the traditional view of dust input, the iron transported by intermediate waters should be consider as an important source of iron for phytoplankton blooms in the Oyashio region. In future studies, quantitative evaluation is necessary for these sources, 1) intermediate water iron transportation, 2) airborne dust iron supply, 3) surface lateral transport, to understand the influence of iron to biological production in the WSP. Our findings contribute to a better understanding of the mechanisms influencing biological production and iron biogeochemical cycles in the subarctic Pacific as well as defining the role of its marginal sea, the Sea of Okhotsk.

Acknowledgements. We express our appreciation and thanks to Dr. T. Kusakabe for support during observations in the Sea of Okhotsk. Thanks are also extended to the crew and officers of *R/V MIRAI*, *Hokko-maru*, *Oshyoro-maru, Wakataka-maru, Hakuho-maru* for their assistance. Anonymous reviewer's comments improved the manuscript. This work was supported by the Central Research Institute of Electric Power Industry, the Ministry of Education, Science and Culture, and the Fisheries Agency

521 research funding, and is a contribution to the Amur-Okhotsk Project, promoted by the Research Institute
522 for Humanity and Nature (RIHN).

523

524 **References**

525 Alfultis, M. A., and S. Martin (1987), Satellite passive microwave studies of the Sea of
526 Okhotsk ice cover and its relation to oceanic processes, 1978-1982, *J. Geophys. Res*.,
527 92. 13,013-13,028.

528 Amakawa, H., Y. Nozaki, D. S. Alibo, J. Zhang, K. Fukugawa, and H. Nagai (2004),
529 Neodymium isotopic variations in Northwest Pacific waters, *Geochim. Cosmochim.*
530 *Acta,,* 68 (4), 715-727.

531 Aumont, O., E. Maier-Reimer, S. Blain, and P. Monfray (2003), An ecosystem model of
532 the global ocean including Fe, Si, P colimitations, *Global Biogeochem. Cycles,* 17(2)
533 1060, doi:10.1029/2001GB001745.

534 Baker, A. R., T. D. Jickells, M. Witt, and K. L. Linge (2006), Trends in the solubility of
535 iron, aluminum, manganese and phosphorus in aerosol collected over the Atlantic
536 Ocean, *Mar. Chem.,* 98, 43-58.

537 Boyd, P.W. et al. (2004), The decline and fate of an iron-induced subarctic
538 phytoplankton bloom, *Nature* 428. 549-553.

539 Boyd, P. W., and P. J. Harrison (1999), Phytoplankton dynamics in the NE subarctic
540 Pacific, *Deep Sea Res. II,* 46. 2405-2432.

541 Boyle, E. A., B. A. Bergquist, R. A. Kayser, and N. Mahowald (2005), Iron, manganese,
542 and lead at Hawaii Ocean Time-series station ALOHA: Temporal variability and an
543 intermediate water hydrothermal plume, *Geochim. Cosmochim. Acta,* 69(4), 933-
544 952.

545 Brown, M. T., W. M. Landing, and C. I. Measures (2005), Dissolved and Particulate Fe
546 in the western and central North Pacific: Results from the 2002 IOC Cruise,
547 *Geochem. Geophys. Geosyst.*, 6, Q10001, doi:10.1029/2004GC000893.

548 Bruland, K. W., E. L. Rue, G. J. Smith, and G. R. DiTullio (2005), Iron, macronutrients
549 and diatom blooms in the Peru upwelling regime: brown and blue waters of Peru,
550 *Mar. Chem.*, 93. 81-103.

551 Buck, C. S., W. M. Landing, J. A. Resing, and G. T. Lebon (2006), Aerosol iron and
552 aluminum solubility in the northwest Pacific Ocean: Results from the 2002 IOC
553 cruise, *Geochem. Geophys. Geosyst.,* 7, Q04M07, doi:10.1029/2005GC000977.

554 Chase, Z., B. Hales, T. J. Cowles, R. Schwartz, and A. van Green (2005), Distribution
555 and variability of iron input to Oregon coastal waters during the upwelling season, *J.*
556 *Geophys. Res.,* 110, C10S12, doi:10.1029/2004JC002590.

557 Croot, P. L., and K. A. Hunter (1998), Trace metal distributions across the continental
558 shelf near Otago Peninsula, New Zealand, *Mar. Chem.,* 62, 185-201.

559 Croot, P. L., K. Andersson, M. Öztürk, and D. R. Turner (2004), The distribution and
560 speciation of iron along 6 ºE in the Southern Ocean, *Deep Sea Res. II,* 51, 2857-2879.

561 Duce, R. A., and N. W. Tindale (1991), Atmospheric transport of iron and its deposition
562 in the ocean, *Limnol. Oceanogr.,* 36, 1715-1726.

563 Duggen, S., P. Croot, U. Schacht, and L. Hoffmann (2007), Subduction zone volcanic
564 ash can fertilize the surface ocean and stimulate phytoplankton growth: Evidence
565 from biogeochemical experiments and satellite data, *Geophys. Res. Letters,* 34,
566 LO1612, doi:10.1029/2006GL027522.

567 Elrod, V. A., W. M. Berelson, K. H. Coale, and K. S. Johnson (2004), The flux of iron
568 from continental shelf sediment: A missing source for global budget, *Geophys. Res.*
569 *Letters,* 31, L12307, doi:10.1029/2004GL020216.

570 Fujishima, Y., K. Ueda, M. Maruo, E. Nakayama, C. Tokutome, H. Hasegawa, M.
571 Matsui, and Y. Sohrin (2001), Distribution of trace bioelements in the subarctic
572 North Pacific Ocean and the Bering Sea (the R/V Hakuho Maru Cruise KH-97-2), *J.*
573 *Oceanogr.,* 57, 261-273.

574 Fung, I. Y., S. K. Meyn, I. Tegen, S. C. Doney, J. G. John, and J. K. B. Bishop (2000),
575 Iron supply and demand in the upper ocean, *Global Biogeochem. Cycles,* 14. 281-
576 291.

577 Gladyshev, S., S. Martin, S. Riser, and A. Figurkin (2000), Dense water production on
578 the northern Okhotsk shelves: Comparison of ship-based spring-summer
579 observations for 1996 and 1997 with satellite observations, *J. Geophys. Res.*, 105.
580 26,281-26,299.

581 Hansell, D. A., C. A. Carlson, and Y. Suzuki (2002), Dissolved organic carbon export
582 with North Pacific Intermediate Water formation, *Global Biogeochem. Cycles*, 16(1),
583 1007, doi10.1029/2000GB001361.

584 Harrison, P. J., F. A. Whitney, A. Tsuda, H. Saito, and K. Tadokoro (2004), Nutrient
585 and Plankton Dynamics in the NE and NW Gyres of the Subarctic Pacific Ocean, *J.*
586 *Oceanogr.*, 60, 93-117.

587 Hernes, P. J., and R. Benner (2002), Transport and diagenesis of dissolved and
588 particulate terrigenous organic matter in the North Pacific Ocean, *Deep-Sea Res. I*,
589 49, 2119-2132.

590 Itoh, M., K. I. Ohshima, and M. Wakatsuchi (2003), Distribution and formation of
591 Okhotsk Sea Intermediate Water. An analysis of isopycnal climatological data, *J.*
592 *Geophys. Res,.*108(C8). 3258, doi:10.1029/2002JC001590.

593 Japan meteorogical agency observed data, http://www.data.kishou.go.jp/obs-
594 env/kosahp/kosa_table_1.html

595 Jickells, T. D., and L. J. Spokes (2001), Atmospheric iron inputs to the Oceans, The
596 *Biogeochemistry of Iron in Seawater*, 85-121.

597 Jickells, T. D. et al. (2005), Global iron connections between desert dust, ocean
598 biogeochemistry, and climate, *Science* 308, 67-71.

599 Johnson, K. S., F. P. Chavez, and G. E. Frederich (1999), Continental-shelf sediment as
600 a primary source of iron for coastal phytoplankton, *Nature* 398. 697-700.

601 Johnson, K. S., R. M. Gordon, and K. H. Coale (1997), What controls dissolved iron
602 concentrations in the world ocean?, *Mar. Chem.*, 57, 137-161.

603 Johnson, K. S. et al. (2007), Developing standards for dissolved iron in seawater. *EOS,*
604 88 (11), 131-132.

605 Johnson, W. K., L. A. Miller, N. E. Sutherland, and C. S. Wong (2005), Iron transport
606 by mesoscale Haida eddies in the Gulf of Alaska, *Deep-Sea Research II* 52. 933-953.

607 Kimura, N., and M. Wakatsuchi (2000), Relationship between sea-ice motion and
608 geostrophic wind in the Northen Hemishphere, *Geophys. Res. Lett.,* 27. 3735-3738.

609 Kinugasa M, T. Ishita , Y. Sohrin , K. Okamura , S. Takeda , J. Nishioka, and A. Tsuda
610 (2005), Dynamics of trace metals during the subarctic Pacific iron experiment for
611 ecosystem dynamics study (SEEDS2001), *Progress in* Oceanography, 64, 129-147.

612 Lam, P. J., J. K. B. Bishop, C. C. Henning, M. A. Marcus, G. A. Waychunas, and I. Y.
613 Fung (2006), Wintertime phytoplankton bloom in the subarctic Pacific supported by
614 continental margin iron, *Grobal Biogeochem. Cycles* 20, GB1006,
615 doi:10.1029/2005GB002557.

616 Löscher, B. M., H. J. W. De Baar, J. T. M. De Jong, C. Veth, and F. Dehairs (1997),
617 The distribution of Fe in the Antarctic Circumpolar Current, *Deep-Sea Res.* II, 44,
618 143-187.

619 Martin, S., R. Drucker, and K. Yamashita (1998), The production of ice and dense shelf
620 water in the Okhotsk Sea polynyas, *J. Geophys Res.,* 103, 27,771-27,782.

621 Martin, J. H., R. M. Gordon, S. Fitzwater, and W. W. Broenkow (1989), VERTEX:
622 phytoplankton/iron studies in the Gulf of Alaska, *Deep-Sea Res. I,* 36(5), 649–680.

623 Mitsudera, H., B. Taguchi, Y. Yoshikawa, H. Nakamura, T. Waseda, and T. Qu (2004),
624 Numerical Study on the Oyashio Water Pathways in the Kuroshio-Oyashio
625 Confluence, *J. Physic. Oceanogr*., 34, 1174-1196.

626 Moore, J. K., S. C. Doney, D. M. Glover, and I. Y. Fung (2002), Iron cycling and
627 nutrient-limitation patterns in surface waters of the World Ocean, *Deep-Sea Res. II*
628 49. 463-507.

629 Measures, C. I., M. T. Brown, and S. Vink (2005), Dust deposition to the surface waters
630 of the western and central North Pacific inferred from surface water dissolved
631 aluminium concentrations, *Geochem. Geophys. Geosyst.,* 6, Q09M03,
632 doi:10.1029/2005GC000922.

633 Nakamura. T., and T. Awaji (2004), Tidally induced diapycnal mixing in the Kuril
634 Straits and its role in water transformation and transport: A three-dimensional
635 nonhydrostatic model experiment, *J. Geophys. Res.,* 109, C09S07,
636 doi:10.1029/2003JC001850.

637 Nakamura, T., T. Toyoda, Y. Ishikawa, and T. Awaji (2006), Effect of tidal mixing at
638 the Kuril Straits on North Pacific ventilation: Adjustment of the intermediate layer
639 revealed from numerical experiments, *J. Geophy. Res.,* 111, C4, C04003,
640 10.1029/2005JC003142.

641 Nakatsuka, T., C. Yoshikawa, M. Toda, K. Kawamura, and M. Wakatsuchi (2002), An
642 extremely turbid intermediate water in the Sea of Okhotsk: Implication for the
643 transport of particulate organic matter in a seasonally ice-bound sea, *Geophys. Res.*
644 *Lett.*, 29, 16, 1757, 10.1029/2001GL014029.

645 Nakatsuka, T., M. Toda, K. Kawamura, and M. Wakatsuchi (2004), Dissolved and
646 particulate organic carbon in the Sea of Okhotsk: Transport from continental shelf to
647 ocean interior, *J. Geophys. Res*., 109, C09S14, doi:10.1029/2003JC001909.

648 Nishioka, J., S. Takeda, C. S. Wong, and W. K. Johnson (2001), Size-fractionated iron
649 concentrations in the northeast Pacific Ocean: distribution of soluble and small
650 colloidal iron, *Mar. Chem*. 74. 157-179.

651 Nishioka, J., S. Takeda, I. Kudo, D. Tsumune, T. Yoshimura, K. Kuma, and A. Tsuda,
652 (2003), Size-fractionated iron distributions and iron-limitation processes in the
653 subarctic NW Pacific, *Geophys. Res. Letters*, 30, 14, 1730,
654 doi:10.1029/2002GL016853.

655 Obata, H., H. Karatani, and E. Nakayama (1993), Automated determination of iron in
656 seawater by chelating resin concentration and chemiluminescence detection, *Anal.*
657 *Chem.*, 65, 1524 – 1528.

658 Obata, H., H. Karatani, M. Matsui, and E. Nakayama (1997), Fundamental studies for
659 chemical speciation of iron in seawater with an improved analytical method. *Mar.*
660 *Chem.*, 56: 97-106.

661 Saito, H., A. Tsuda, and H. Kasai (2002), Nutrient and plankton dynamics in the
662 Oyashio region of the western subarctic Pacific, *Deep-Sea Res. II,* 49. 5463-5486.

663 Sarmiento, J. L., G. Thiele, R. M. Key, and W. S. Moore (1990), Oxygen and nitrate
664 new production and remineralization in the North Atlantic subtropical gyre, *J.*
665 *Geophys Res.*, 95, C10, 18303-18315.

666 Suga, T., K. Motoki, and Y. Aoki (2004), The North Pacific climatology of winter
667 mixed layer and mode waters, *J. Phys. Oceanogr*. **34**. 3-22.

668 Takahashi, T., S. C. Sutherland, C. Sweeney, A. Poisson, N. Metzl, B. Tilbrook, N.
669 Bates, R. Wanninkhof, R. A. Feely, C. Sabine, J. Olafsson, and Y. Nojiri (2002),

Global sea-air CO_2 flux based on climatological surface ocean pCO_2, and seasonal biological and temperature effects, *Deep-Sea Res. II*, 49, 1601-1622.

Talley, L. D. (1991), An Okhotuk Sea water anomaly: Implications for ventilation in the North Pacific, *Deep Sea Res.,I,* 38, S171-S190.

Tsuda, A. et al. (2003), A mesoscale iron enrichment in the western subarctic Pacific induces large centric diatom bloom, *Science* 300, 958-961.

Tsurushima, N., Y. Nojiri, K. Imai, and S. Watanabe (2002), Seasonal variations of carbon dioxide system and nutrients in the surface mixed layer at station KNOT (44N, 155E) in the subarctic western North Pacific, *Deep-Sea Res. II*, 49, 5377-5394.

Uematsu, M., et al. (1983), Transport of mineral aerosol from Asia over the North Pacific Ocean, *J. Geophys. Res.*, 88, 5343-5352.

Uematsu, M., Z, Wang, and I. Uno (2003), Atmospheric input of mineral dust to the western North Pacific region based on direct measurements and regional chemical transport model, *Gephys. Res. Letters* 30, 6, 1342, doi:10.1029/2002GL016645.

Watanabe, Y. W., K. Harada, and K. Ishikawa (1994), Chlorofluorocarbons in the central North Pacific and southward spreading time of North Pacific intermediate water, *J. Geophys. Res.* 99, C12, 25195-25214.

Wells, M. L., and L. M. Mayer (1991), Variations in the chemical lability of iron in estuarine, coastal and shelf waters and its implications for phytoplankton, *Mar. Chem.* 32, 195-210.

Wells, M. L., G. K. Vallis, and E. A. Silver (1999), Tectonic processes in Papua New Guinea and past productivity in the eastern equatorial Pacific Ocean, *Nature* 398, 601-604.

693 Wong, C. S., R. J. Matear, H. J. Freeland, F. A. Whitney, and A. S. Bychkov (1998),
694 WOCE line P1W in the sea of Okhotsk: 2. CFCs and the formation rate of
695 intermediate water, *J. Geophys, Res*., 103. 15,625-15,642.

696 Wu, J., and G. W. Luther (1996), Spatial and temporal distribution of iron in the surface
697 water of the northwestern Atlantic Ocean, *Geochim. Cosmochim. Acta,* 60, 2729-
698 2741.

699 Yamamoto-Kawai, M., S. Watanabe, S. Tsunogai, and M. Wakatsuchi (2004),
700 Chlorofluorocarbons in the Sea of Okhotsk: Ventilation of the intermediate water, *J.*
701 *Gophys. Res*., 109, C09S11, doi:10.1029/2003JC001919.

702 Yamamoto, M., S. Watanabe, and S. Tsunogai (2002), Effect of sea ice formation and
703 diapycnal mixing on the Okhotsk Sea Intermediate Water clarified with oxygen
704 isotopes, *Deep Sea Res*., 49, 1165-1174.

705 Yasuda, I. (1997), The origin of the North Pacific Intermediate Water, *J. Geophys. Res*.
706 102 (C1). 893-909.

707 Yasuda, I., Y. Hiroe, K. Komatsu, K. Kawasaki, T. M. Joyce, F. Bahr, and Y. Kawasaki
708 (2001), Hydrographic structure and transport of the Oyashio south of Hokkaido and
709 the formation of North pacific Intermediate Water, *J. Geophys. Res*., 106(C4), 6931-
710 6942.

711 Yoshikawa, C., T. Nakatsuka, and M. Wakatsuchi (2006), Distribution of N* in the Sea
712 of Okhotsk and its use as a biogeochemical tracer of the Okhotsk Sea Intermediate
713 Water formation process, *Journal of Marine Systems*. 63, 49-62

714

715

716

716 **Figure caption**

717 Figure 1. Chart of the subarctic Pacific area with sampling locations in this study.
718 Stations indicated by filled triangles are observed total dissolvable iron and dissolved
719 iron concentrations in May to June, 2000 cruise. Time-series observations were
720 conducted from January to the end of May in 2003 at stations along "*A-line*", which are
721 indicated by filled circles. Spatial observations were conducted in April and May 2003
722 at stations indicated by open circles. Time-series observations were also conducted at
723 station B9. A longitudinal vertical section observation in the North Pacific along 165º E
724 were carried out, at the stations indicated by the filled squares, in September 2003.
725 Arrows indicate a schematic image of the intermediate water currents (dashed line) and
726 surface water currents (solid line). DSW=Dense Shelf Water; OSIW=Okhotsk Sea
727 Intermediate Water; OY=Oyashio; KR=Kuroshio.

728

729 Figure 2. a, Vertical profiles of Total dissolvable iron (TD-Fe), dissolved iron (D-Fe)
730 and dissolved oxygen in the, a, WSP (western subarctic Pacific), b, the Oyashio region
731 and, c, the Sea of Okhotsk.

732

733 Figure 3. a, Total dissolvable iron (TD-Fe) versus water density plot (right) around the
734 Kuril Island. Green symbols indicate the data from the Sea of Okhotsk, red symbols
735 indicate the data from the Oyashio region and blue symbols indicate the data from
736 oceanic regions of the WSP. b, Dissolved iron (D-Fe) D-Fe versus water density plot
737 around the Kuril Island. All symbols are same as "a".

738

739 Figure 4. A longitudinal section of a: salinity, b: dissolved iron and c: total iron profile
740 in the North Pacific along 165º E. Density range of 26.6-27.5 σ_θ is located on each
741 figure.

742

743 Figure 5. Vertical profiles of dissolved iron, total iron, salinity and dissolved oxygen at
744 35 ºN, 165º E.

745

746 Figure 6. Vertical profiles of N* values (filled triangles), and TD-Fe (open circles) and
747 D-Fe (filled circles) at station C1 (at the Sea of Okhotsk: a) and C5 (at the Oyashio
748 region: b).

749

750 Figure 7. Average Total Fe concentrations and average temperatures in the surface
751 mixed layers at stations in the WSP. a: data from the April 2003 cruise, b: data from the
752 May 2003 cruse. C: Iron concentrations are plotted on the map of the WSP. dotted line
753 indicates the subarctic front (SF).

754

755 Figure 8. Vertical profiles of D-Fe, T-Fe and Temperature at station A4 (at north of
756 subarctic front) and B6 (at south of subarctic Front).

757

758 Figure 9. a, Vertical profiles of dissolved iron, total iron, salinity, and nitrate+nitrite,
759 from January to May at stations A7 (Upper stream of Oyashio region) and b, from
760 March to May at station B9 (down stream of Oyashio region) in 2003.

761

762 Figure 10. a, Seasonal variations in sea-surface dissolved iron concentrations (average
763 in surface mixed layer), nitrate+nitrite concentrations (average in surface mixed layer),
764 surface mixed layer depths (MLD) and chlorophyll a concentrations (average in surface
765 mixed layer), from January to the end of May, 2003, along the "*A-line*".

766

767 Figure 11. Dissolved Iron, Nitrate and Temperature profiles at Station A11, B9 and
768 Papa [data from Nishioka et al., 2001] used in the estimations of slopes and mixed layer
769 depth (MLD) shown in Table 2.

770

771 Figure 12. A schematic drawing of evaluated upward iron transport processes. A: by
772 winter mixing, B: by eddy diffusion, C: vertical advection. C_1 is the summer dissolved
773 Fe concentration at the maximum depth of the winter mixed layer. C_2 is dissolved Fe
774 concentration in the summer surface mixed layer. D_1 is the summer surface mixed
775 layer depth. D2 is winter surface mixed layer depth.

776

777 Figure 13. Schematic of iron supply process proposed in this study. Water ventilation
778 processes in this region control the transport of dissolved and particulate iron through
779 the intermediate water layer from the continental shelf of the Sea of Okhotsk to the wide
780 area of the WSP.
781

781

Table 1 Cruise, stations, observed depth range and Fe measurement in this study

Year	Month	Vessel	Cruise	Stations*	Observed minimum and maximum depth(m)	Fe measurement**
2000	May-June	Mirai	MR00K-03	C0, C1, C2, C3, C4, C5, C7, C8, C9, C11, B9	10-5500	TD-Fe, D-Fe
2003	January	Hokko-maru	HK0301	A3, A4, A5, A7, A9, A11, A15	10-800	T-Fe, D-Fe
2003	February	Oshoro-maru	OS131	A7	10-300	T-Fe, D-Fe
2003	March	Oshoro-maru	OS133	A4, A7, B9	10-800	T-Fe, D-Fe
2003	April	Wakataka-maru	WK0304	A4, A7, A11, A17, B1, B2, B3, B4, B5, B6, B7, B8, B9, B14, re-A4, re-A7, re-A11	10-800	T-Fe, D-Fe
2003	May	Wakataka-maru	WK0305	A4, A7, A11, A17, B3, B4, B9, B14 re-A4, re-A7, re-A11	10-800	T-Fe, D-Fe
2003	September	Hakuho-maru	KH03-2	D1, D2, D3, D4, D5	10-5000	T-Fe, D-Fe

* All station are indicated in Figure 1. re-: re-visit
** TD-Fe: Total dissolvable iron (dissolved plus leachable iron at < pH 3.2)
T-Fe: Total iron (dissolved plus leachable iron at < pH 1.8 during more than 1 yr storage)
D-Fe: Total iron (leachable iron in < 0.22 mm at pH 3.2)

782

783

784

785

786

Table. 2 Calculated dissolved iron upwerd flux and iron/nitrate ratio from below surface

	OY (A11)	WSP (B9)	ESP (St.Papa*)
winter max. MLD (m)	200	100	80
summer MLD (m)	20	20	40
dFe/dZ (μmol/m^4)	0.0032	0.0060	0.0017
Dissolved Fe conc. at winter MLD in the summer vertical profile (nM): C1	0.45	0.28	0.11
Dissolved Fe conc. in summer MLD (nM): C2	0.07	0.10	0.09
mean D-Fe concentration at subsurface gradient (nM): R	0.73	0.48	0.17
dN/dZ (mmol/m^4)	0.072	0.115	0.453
dFe(nM)/dN(μM) ratio	0.044	0.052	0.004
Iron amounts transported by winter mixing (μmol Fe/m^2)	7.6	3.6	0.8
Iron amounts transported by eddy diffusion** (μmol Fe/m^2)	3.4	6.5	1.8
Iron amounts transported by vertical advection*** (μmol Fe/m^2)	1.9	1.2	0.4
Total annual upward iron flux (μmol Fe/m^2/yr)	12.9	11.3	3.0

OY: Oyashio region, WSP: western subarctic Pacific region, ESP: eastern subarctic Pacific region
Data in station A11, station B9 and station Papa are shown in Fig. 11.
MLD: surface mixed layer depth
*Station Papa data was refered from Nishioka et al., 2001
** Employed coefficient of eddy diffusivity: Kz = 5m^2/day
*** Employed vertical velocity: W = 0.012 m/day

786

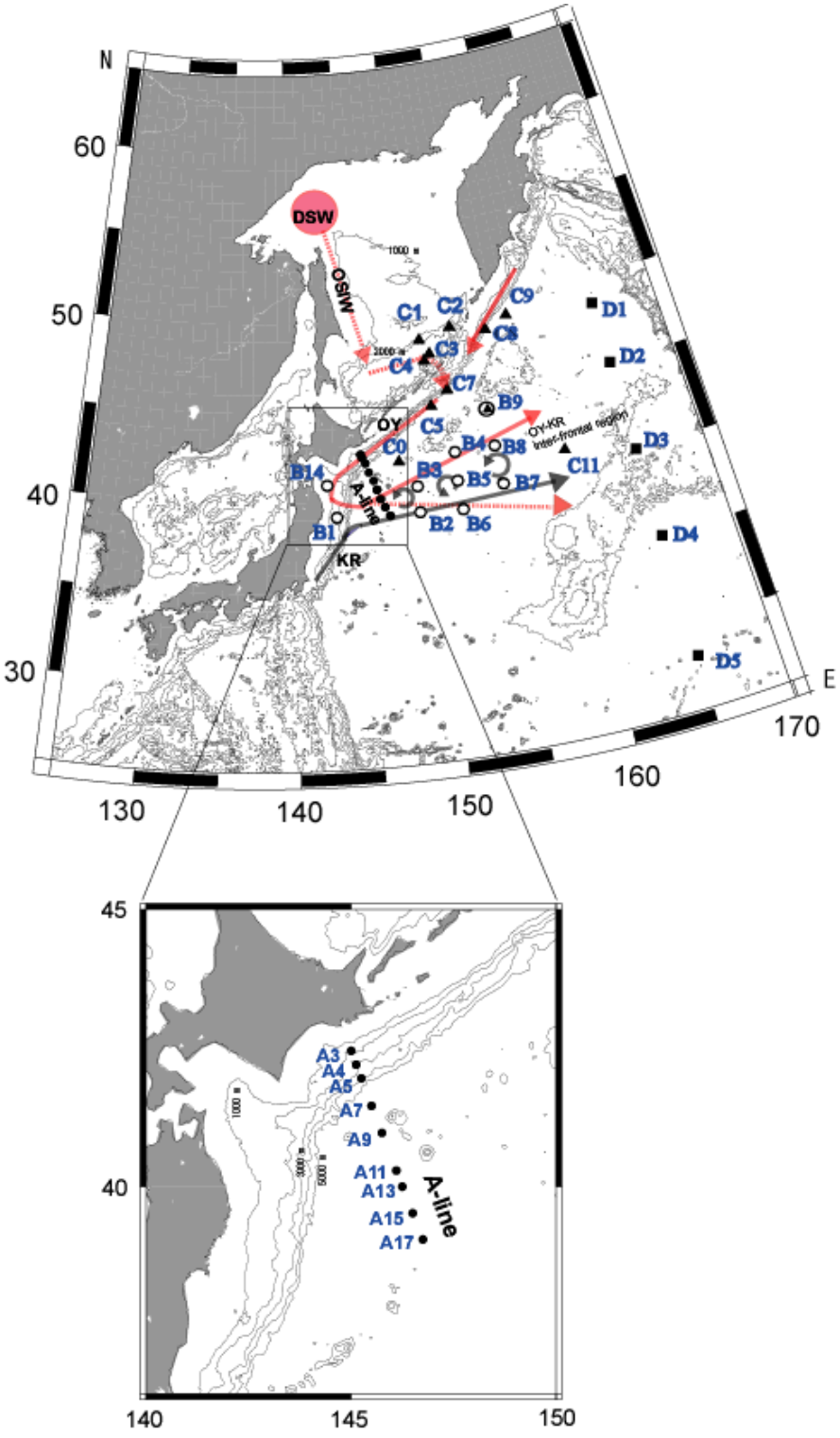

Nishioka et al., Fig.1

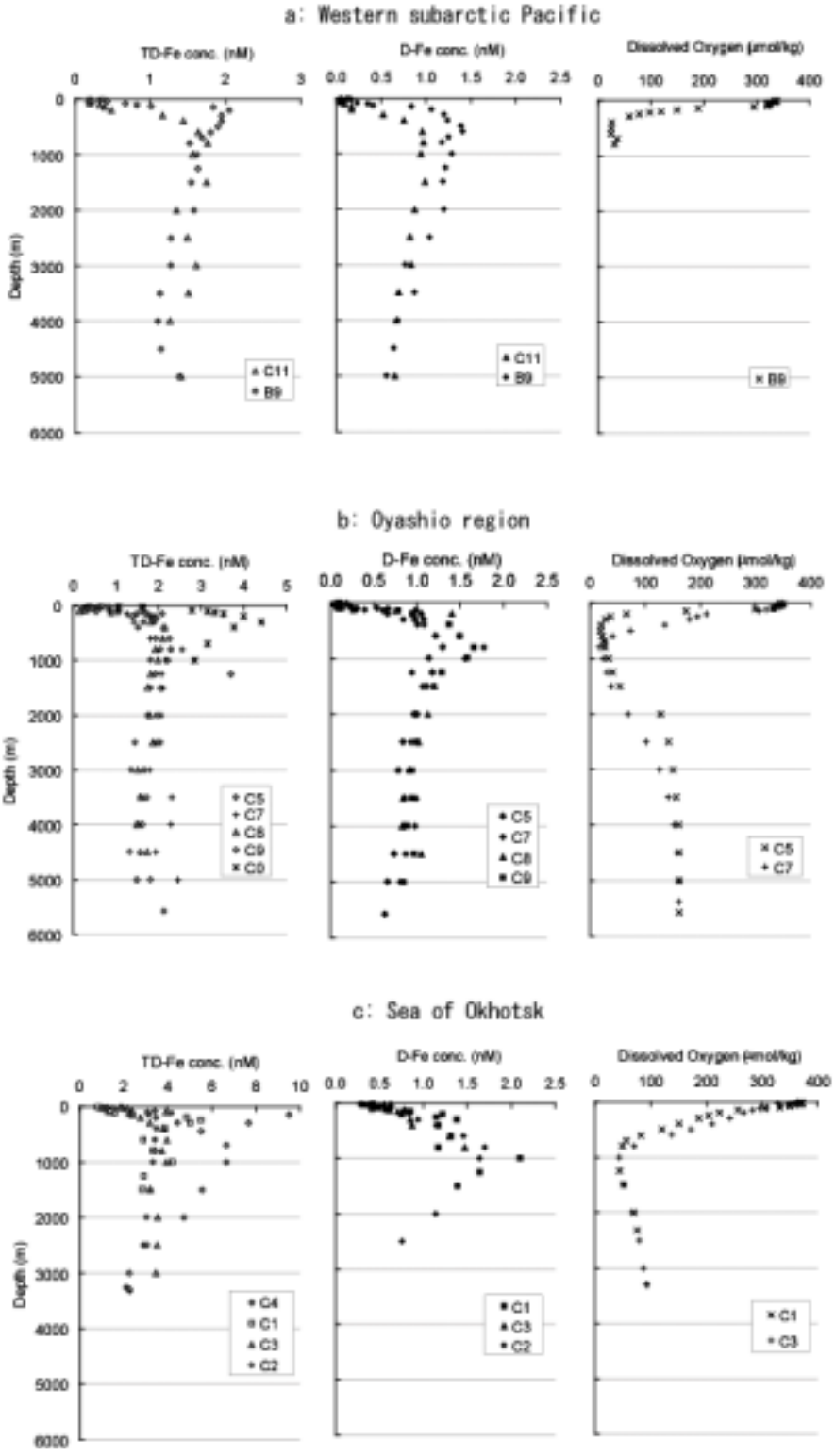

Nishioka et al., Fig. 2

3

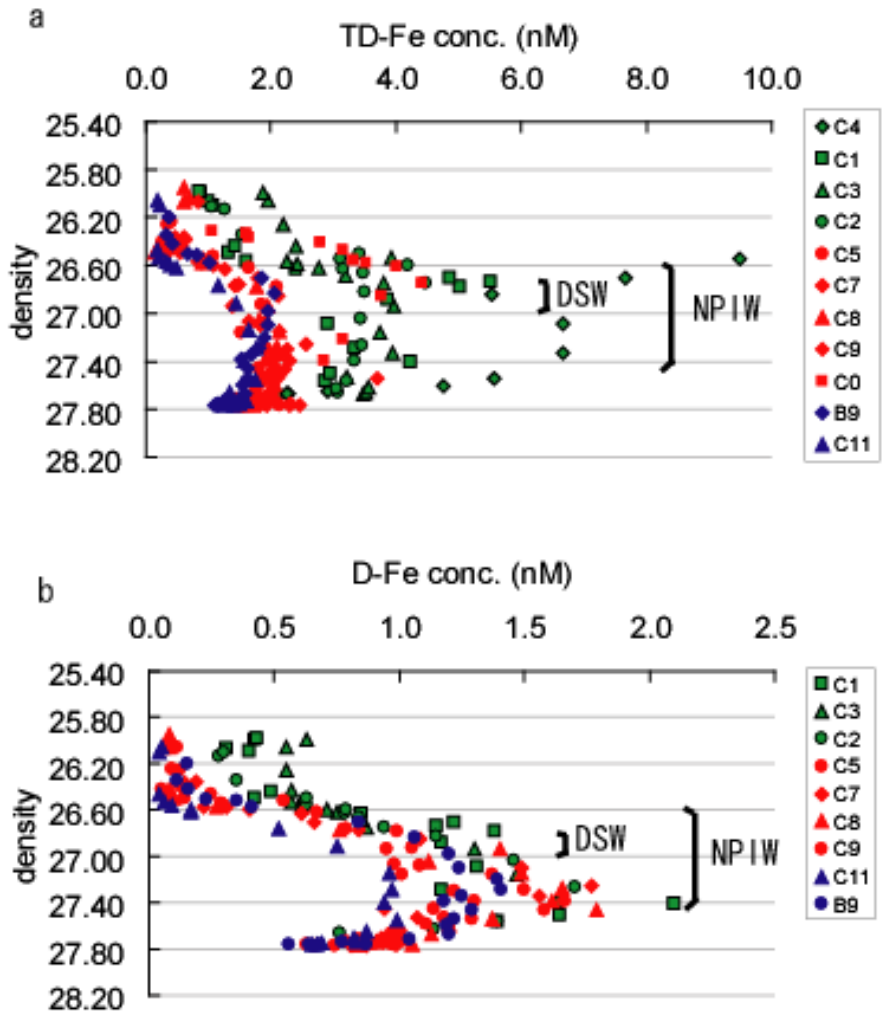

Nishioka et al. Fig. 3

3

4

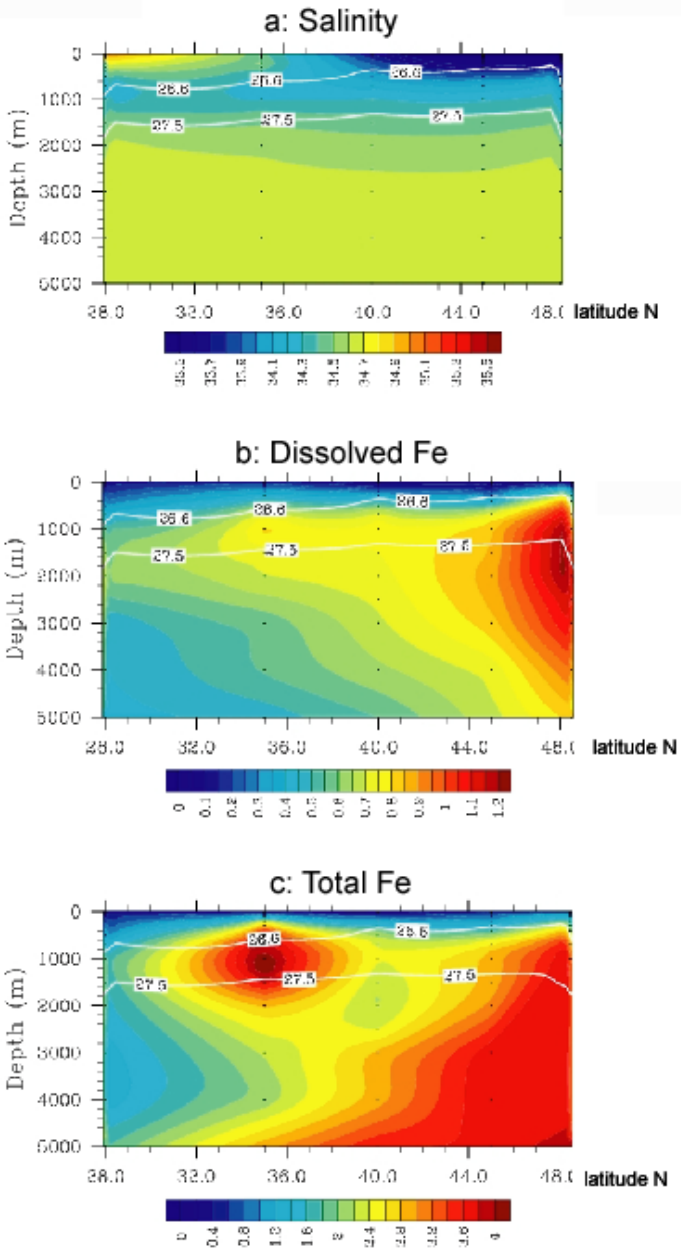

Nishioka et al., Fig. 4

4

5

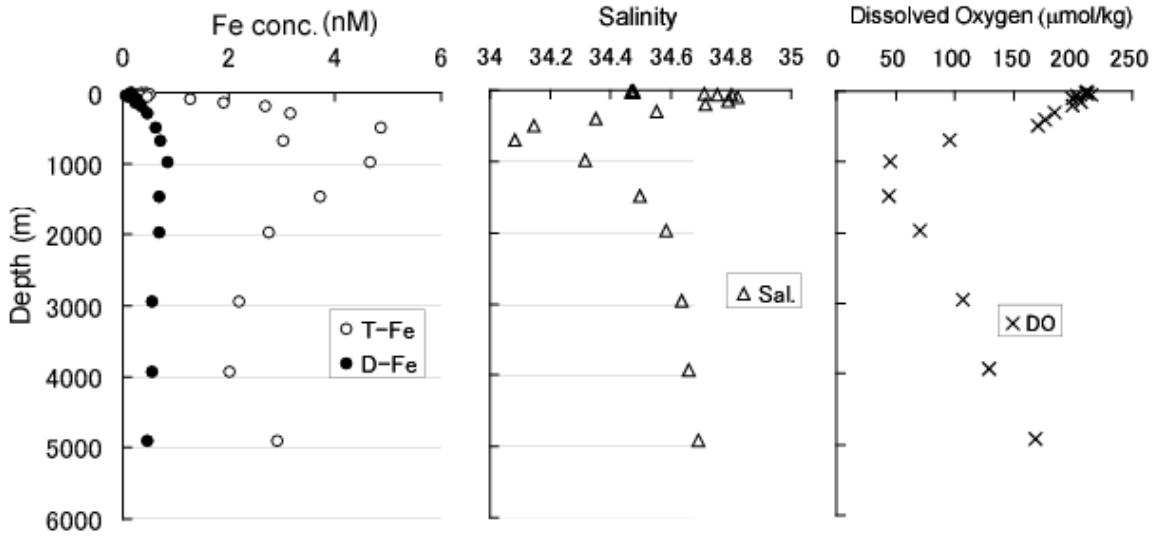

Nishioka et al., Fig. 5

5

6

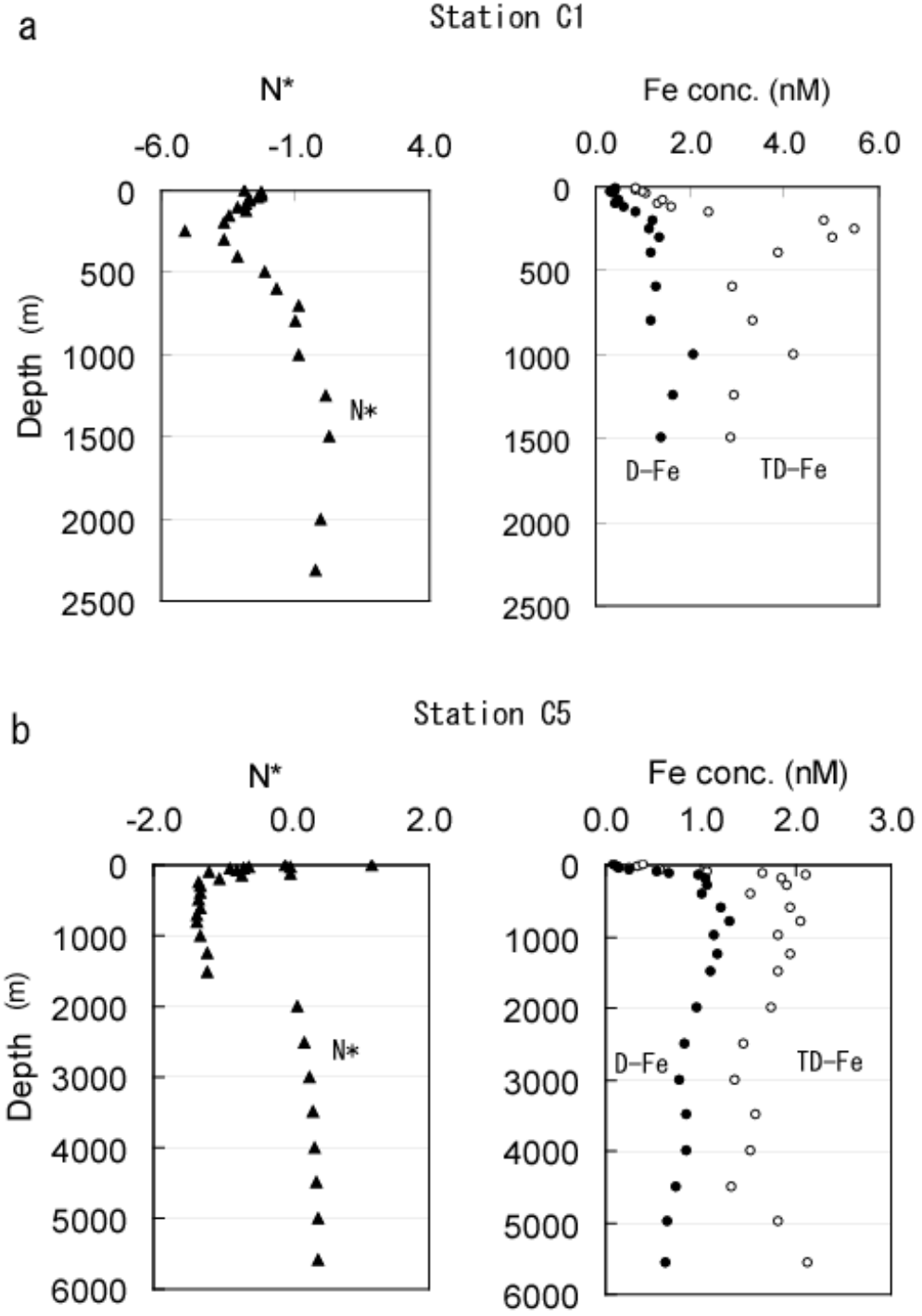

Nishioka et al.Fig. 6

6

7

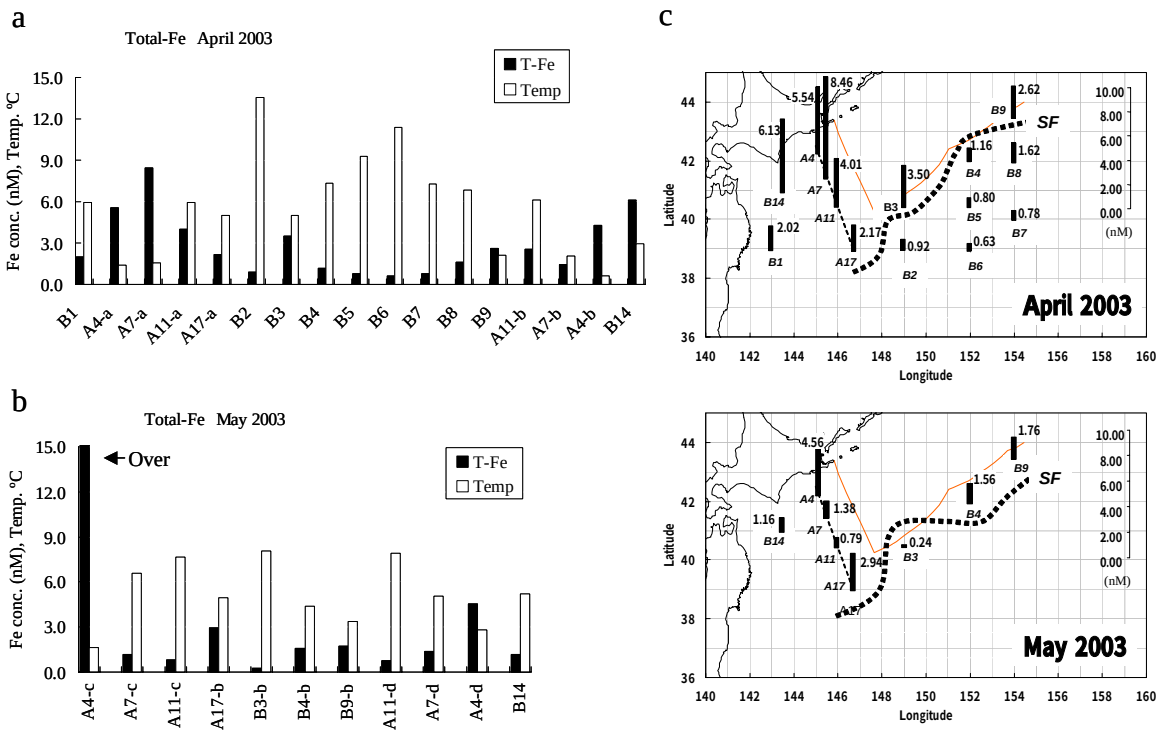

Nishioka et al. Fig. 7

7

8

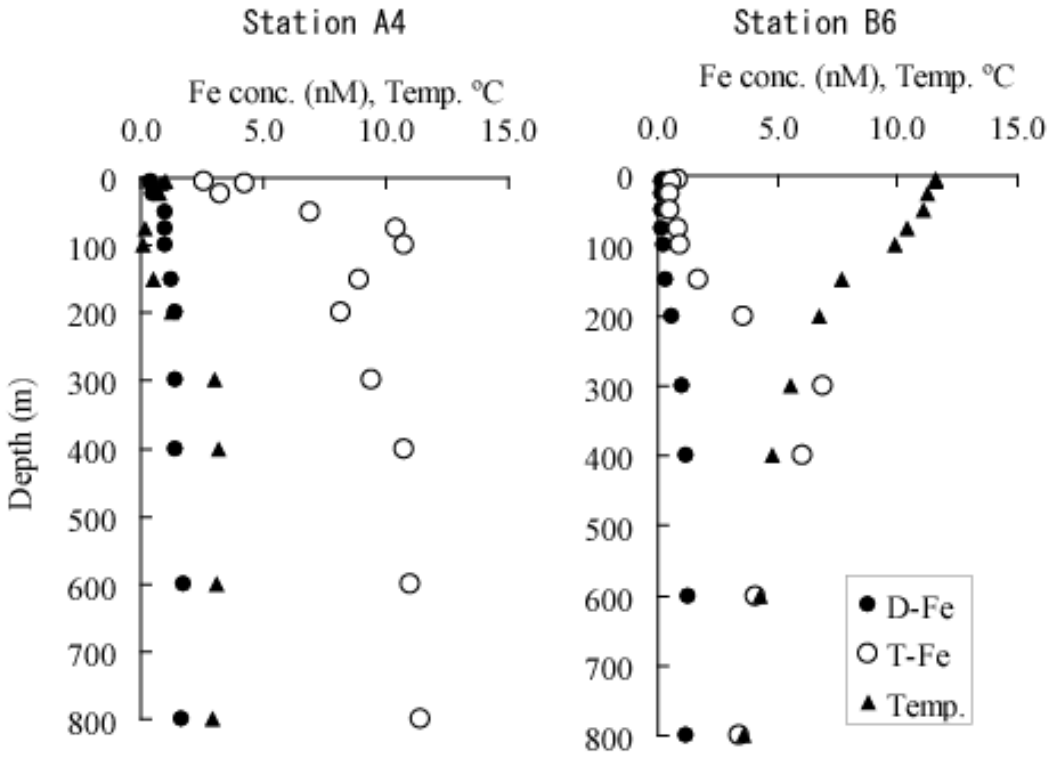

Nishioka et al. Fig. 8

8

9

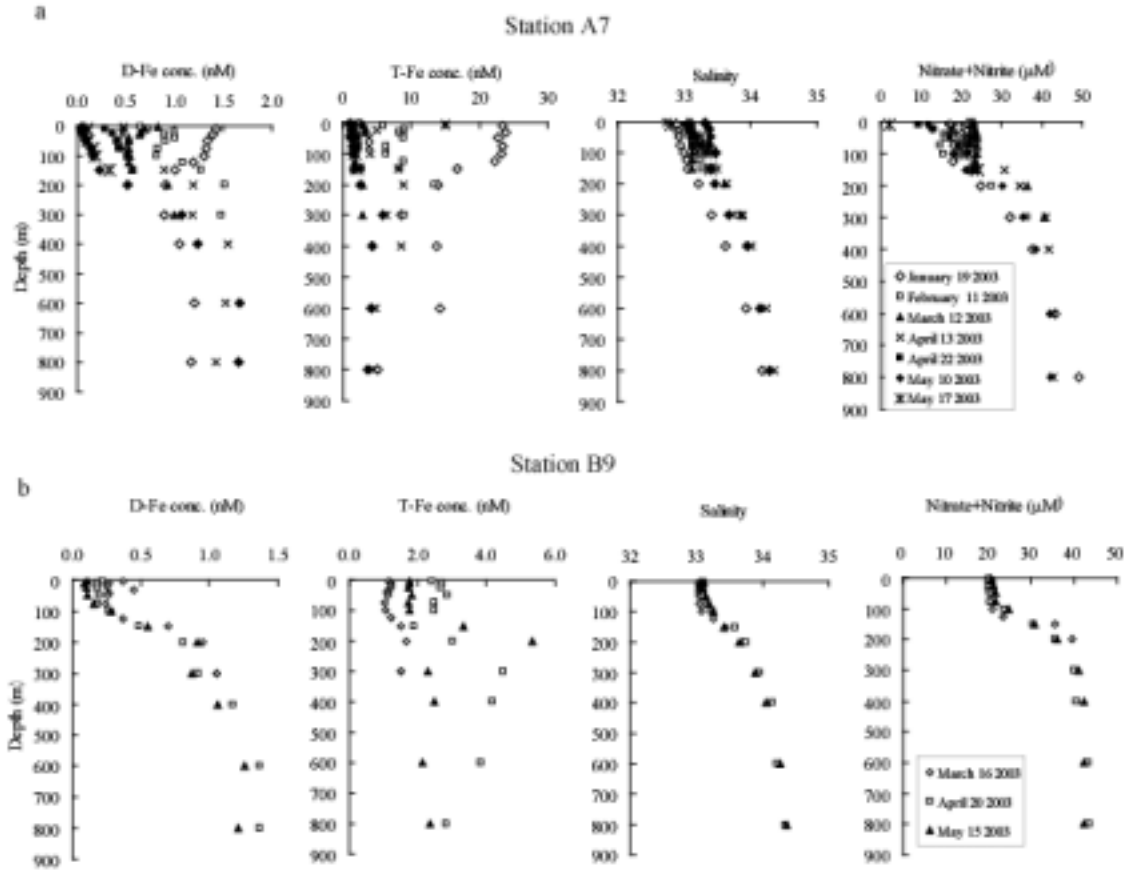

Nishioka et al. Fig. 9

9

10

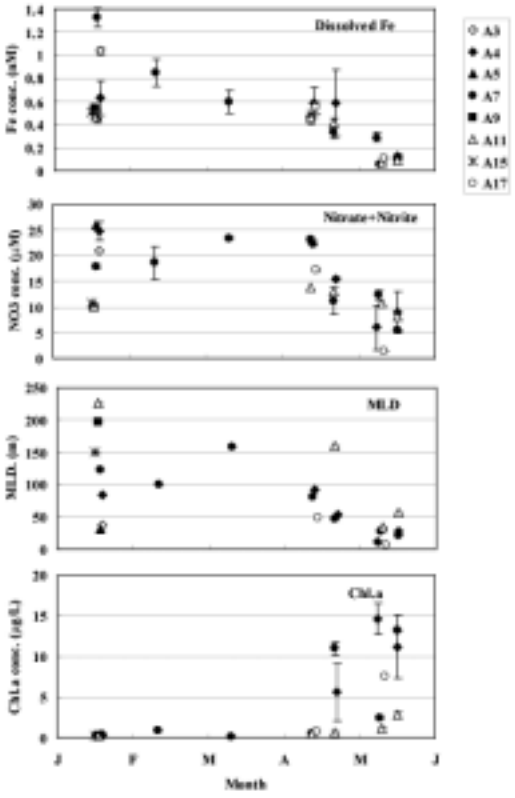

Nishioka et al. Fig. 10

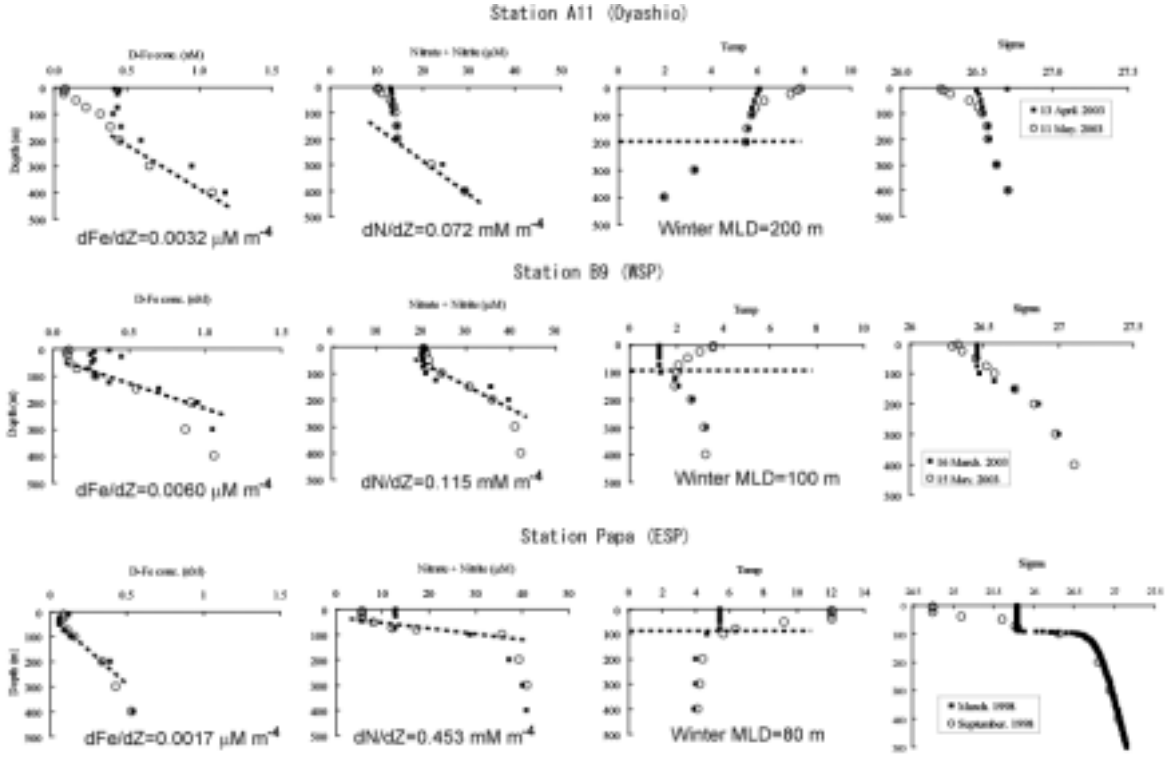

Nishioka et al. Fig. 11

11

12

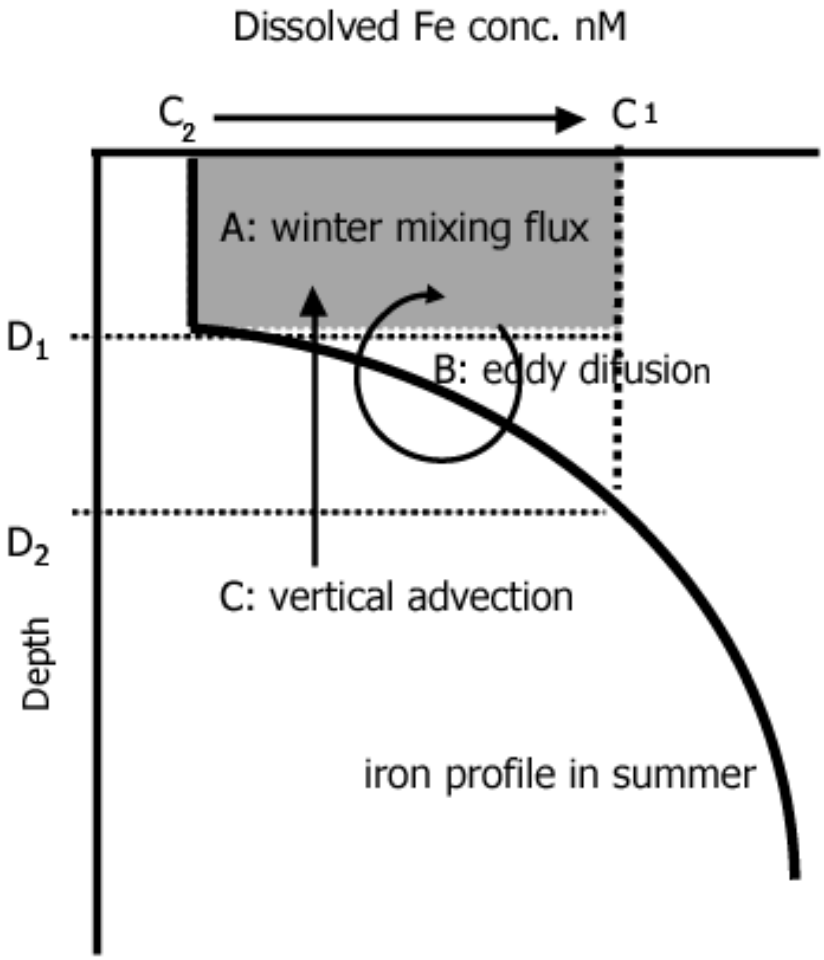

Nishioka et al. Fig. 12

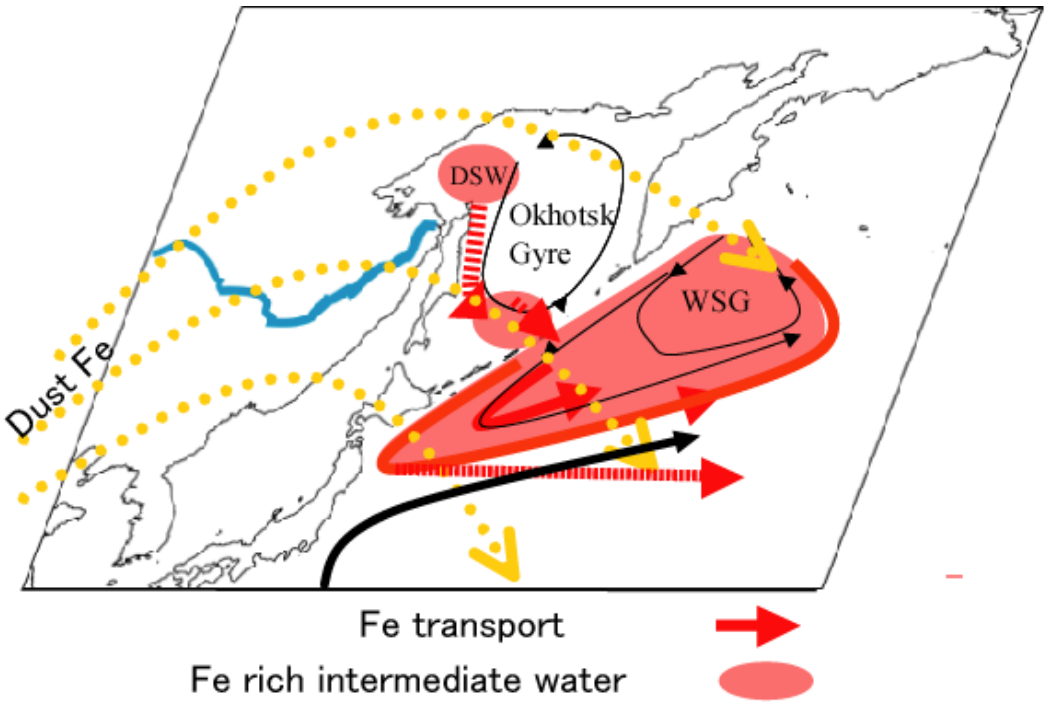

Fe transport

Fe rich intermediate water

Nishioka et al. Fig. 13